Atomic clocks and spectroscopy experiments

Michał Zawada
KL FAMO, Nicolaus Copernicus University

6 January 2020

iqClock
QUANTUM FLAGSHIP
EMPIR
EURAMET
The EMPIR initiative is co-funded by the European Union's Horizon 2020 research and innovation programme and the EMPIR Participating States

Fundusze Europejskie Inteligentny Rozwój
Rzeczpospolita Polska
FNP Fundacja na rzecz Nauki Polskiej
Unia Europejska Europejski Fundusz Rozwoju Regionalnego

La seconde

est la durée de 9 192 631 770 périodes de la radiation correspondant à la transition entre les deux niveaux hyperfins de l'état fondamental de l'atome de césium 133.

The second is the duration of 9 192 631 770 periods of the radiation corresponding to the transition between the two hyperfine levels of the ground state of the caesium 133 atom.

Atomic clock

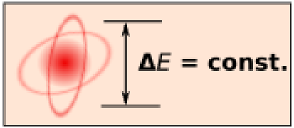

Atomic clock diagram

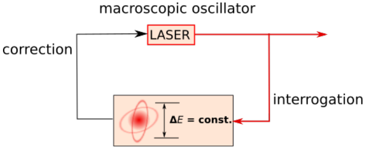

- Ideal clock: a signal with stable and universal frequency.
- Energy levels of unperturbed atoms are stable and universal.

Atomic clock

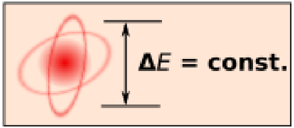

Atomic clock diagram

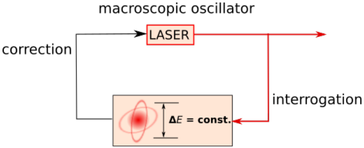

$$\omega(t) = \omega_{ef} * (1 + \varepsilon + y(t))$$

ε -fractional offset of frequency
$y(t)$ - fractional fluctuations of frequency

Accuracy

- uncertainty of ε

Stability

- statistical properties of $y(t)$, characterized by the Allan deviation $\sigma_y(\tau)$

Michał Zawada
KL FAMO, Nicolaus Copernicus University

Accuracy and stability

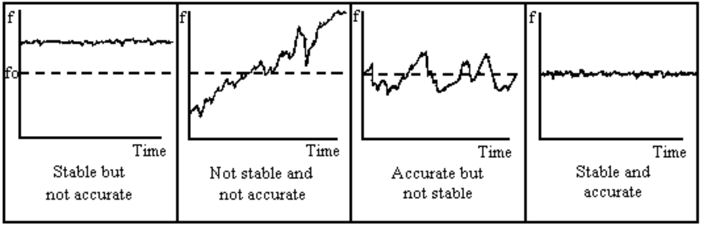

source: nist.gov

Allan deviation Details - Session II

$$\sigma_f(\tau) = \sqrt{\frac{1}{2}\sum_n \frac{\left(f_{n+1,\tau} - f_{n,\tau}\right)^2}{n}}$$

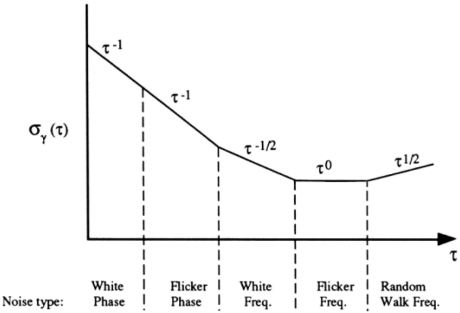

source: nist.gov

f_n is a set of frequency offset measurements that consists of individual measurements, f_1, f_2, f_3, and so on and the data are equally spaced in segments τ seconds long.

Time standards

1. Atomic fountains, **accuracy** of $\sim 10^{-16}$
2. Commercial caesium clocks, with good long term **stability** $\sim 10^{-15}$ over few months and **accuracy** of $\sim 10^{-13}$
3. Hydrogen masers: 1.4 GHz hyperfine structure transition in atomic hydrogen. Much better short-time **stability** than any commercial caesium clock: $\sim 10^{-15}$ over few hours

Caesium clocks and hydrogen masers

HP5071A caesium clock and VCH-1005 hydrogen maser in the Central Office of Measures in Poland

Caesium clocks and hydrogen masers vs optical clock

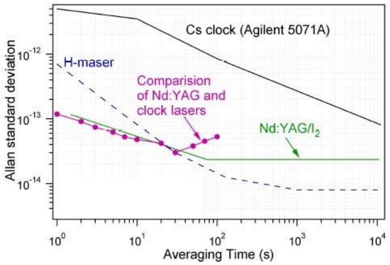

Feng-Lei Hong et al. Opt. Express 13, 5253-5262 (2005)

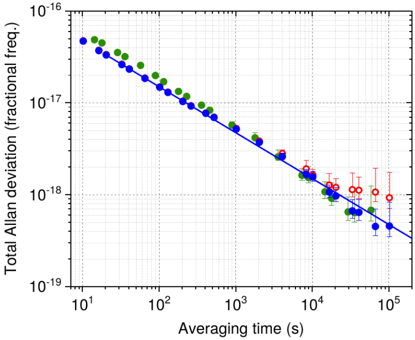

W.F. McGrew et al. Nature 564, 87-90 (2018)

Atomic fountains

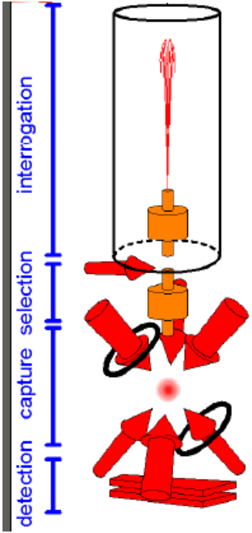

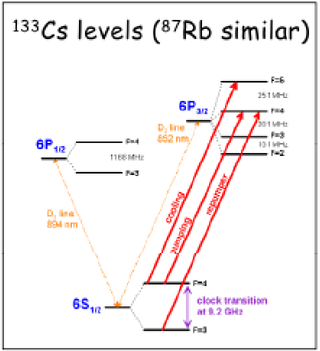

a)

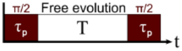

b)

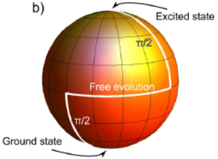

Atomic fountains

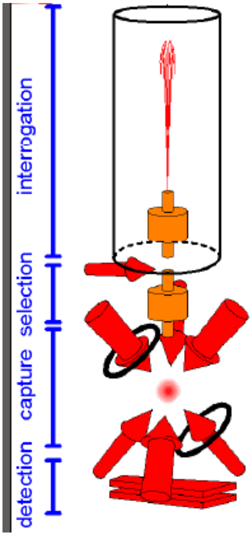

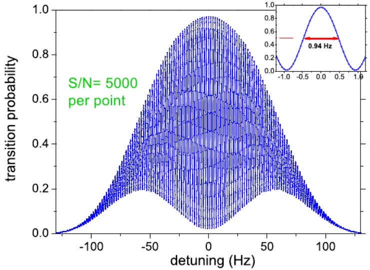

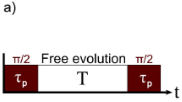

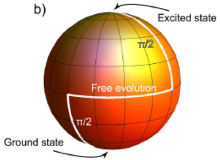

Atomic fountains

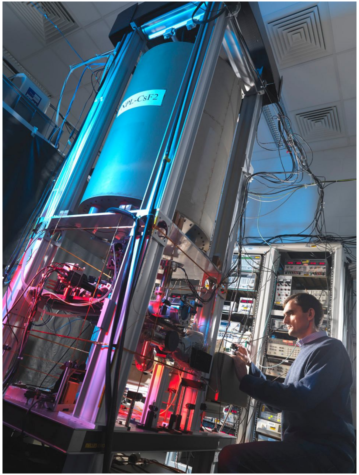

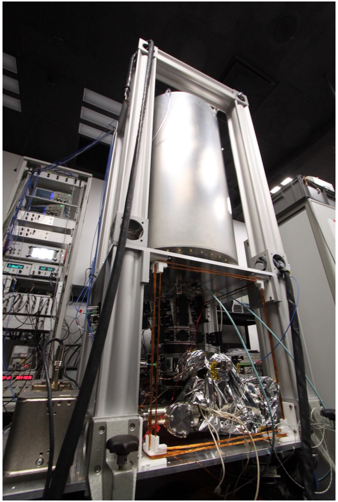

Atomic fountains vs optical clock

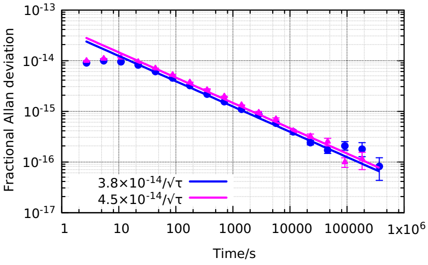

J. Lodewyck et al. Metrologia 53, 1123 (2016)

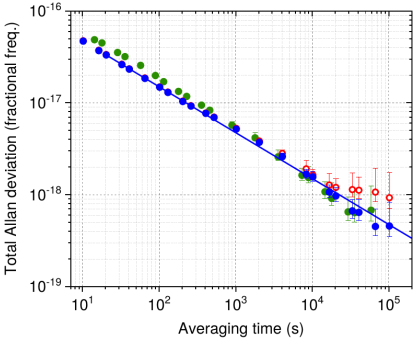

W.F. McGrew et al. Nature 564, 87-90 (2018)

Microwave clocks vs optical clocks

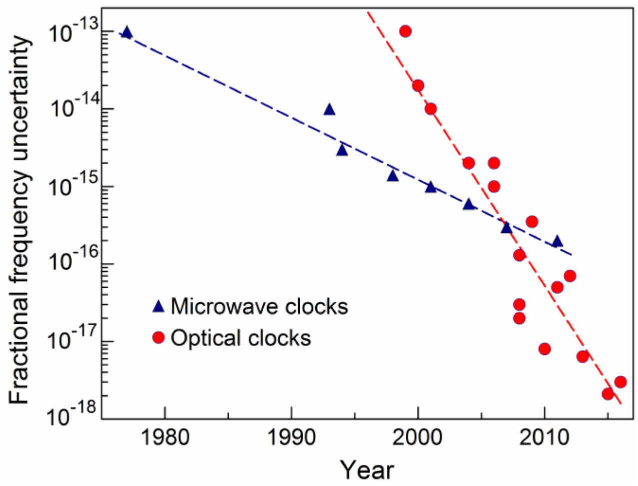

MS Safronova et al., Rev. Mod. Phys. 90, 025008 (2018)

Microwave clocks vs optical clocks

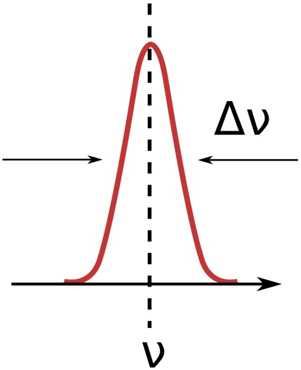

Quality of the clock: $Q = \frac{\nu}{\Delta\nu} \times \frac{S}{N}$

Microwave clocks vs optical clocks

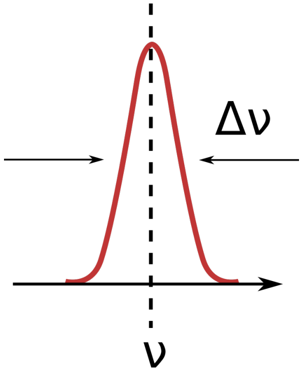

Quality of the clock: $Q = \frac{\nu}{\Delta\nu} \times \frac{S}{N} \sim \nu T \times \frac{S}{N}$

Microwave clocks vs optical clocks

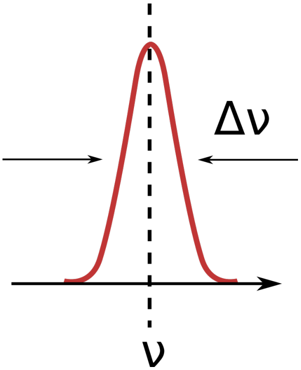

Quality of the clock: $Q = \frac{\nu}{\Delta\nu} \times \frac{S}{N} \sim \nu T \times \frac{S}{N}$

Stability of an atomic clock: $\sigma_y(\tau) \sim \frac{\sigma_{spect}}{Q}\sqrt{\frac{T_c}{\tau}}$

Microwave clocks vs optical clocks

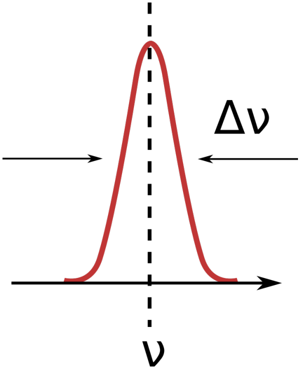

Quality of the clock: $Q = \frac{\nu}{\Delta\nu} \times \frac{S}{N} \sim \nu T \times \frac{S}{N}$

Stability of an atomic clock: $\sigma_y(\tau) \sim \frac{\sigma_{spect}}{Q}\sqrt{\frac{T_c}{\tau}}$

Quantum Shot Noise limitation: $\sigma_y(\tau) = \frac{1}{\pi Q} \times \frac{1}{N_{at}} \times \sqrt{\frac{T_c}{\tau}}$

Optical clocks: trapped ions and neutral atoms

Ion traps: Ions trapped in the Paul trap by the RF field

- Trap is perturbed only slightly $\Rightarrow$ excellent accuracy 9.4×10^{-18}
- Good stability $(1.2 \times 10^{-15}/\sqrt{\tau})$, but restricted by Quantum Shot Nose - only 1 ion

S. M. Brewer et al. 123, 033201 (2019)

Optical clocks: trapped ions and neutral atoms

Ion traps: Ions trapped in the Paul trap by the RF field

- Trap is perturbed only slightly $\Rightarrow$ excellent accuracy 9.4×10^{-18}
- Good stability $(1.2 \times 10^{-15}/\sqrt{\tau})$, but restricted by Quantum Shot Nose - only 1 ion

  S. M. Brewer et al. 123, 033201 (2019)

Neutral atoms: Optical lattice

- A trap with a high-intensity light $\Rightarrow$ high perturbation, though well under control. $2 * 10^{-18}$

  T. Bothwell et al. arXiv:1906.06004 (2019)
- High number of atoms $(10^4)\Rightarrow$ high stability possible. $1.5 \times 10^{-16}/\sqrt{\tau}$ down to 3.2×10^{-19}

  W.F. McGrew et al. Nature 564, 87-90 (2018)

A transition good for optical clock

Natural linewidth of an electric dipole (E1) transition is typically bigger than 1 MHz $\Rightarrow$ Q below 10^8

A transition good for optical clock

Natural linewidth of an electric dipole (E1) transition is typically bigger than 1 MHz $\Rightarrow$ Q below 10^8

Clock transition should be:

- Narrow (forbidden)
- Mostly insensitive to external fields.

A transition good for optical clock

Natural linewidth of an electric dipole (E1) transition is typically bigger than 1 MHz $\Rightarrow$ Q below 10^8

Clock transition should be:

- Narrow (forbidden)
- Mostly insensitive to external fields.

Possible candidates:

- two-photon transitions and higher order electric transitions (quadrupole, octupole . . .)
- a low energy nuclear transition (still sought at ^{229}Th)
- an intercombination transition

Alkaline-earth and alkaline-earth like atoms/ions

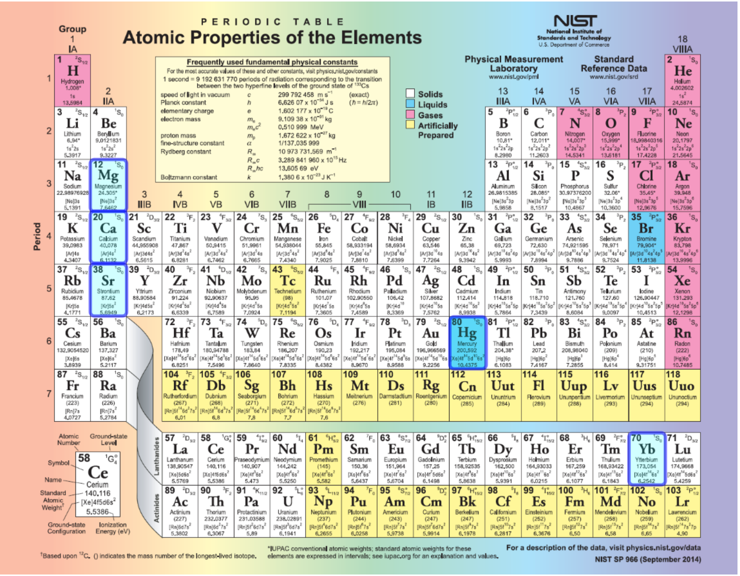

Alkaline-earth and alkaline-earth like atoms/ions

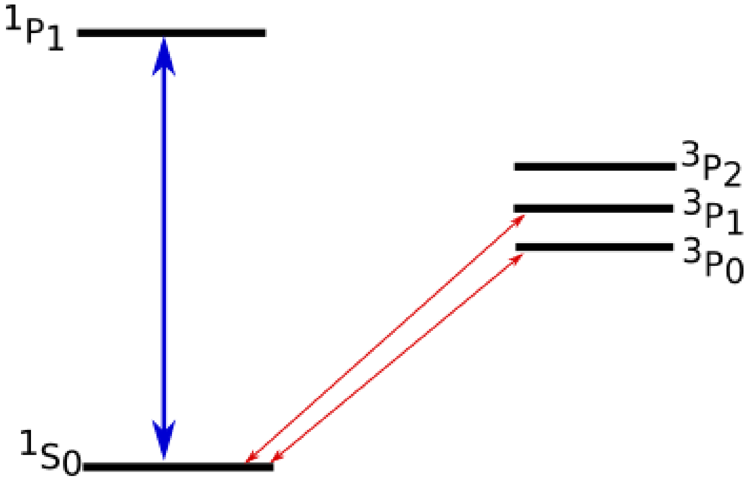

Alkaline-earth and alkaline-earth like atoms/ions

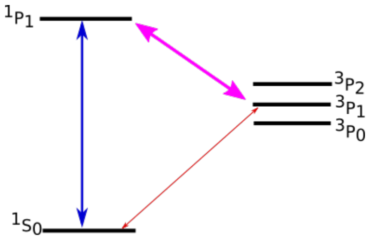

- Forbidden $^1S_0 - {}^3P_1$ transition:
  - Fine structure interaction

Alkaline-earth and alkaline-earth like atoms/ions

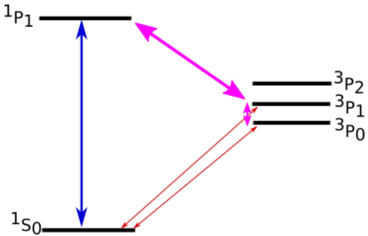

- Forbidden $^1S_0 - {}^3P_1$ transition:
  - Fine structure interaction
- Double forbidden $^1S_0 - {}^3P_0$ transition:
  - Fermions: hyperfine interaction
  - Bosons: quenching by a static B field

Optical atomic clocks

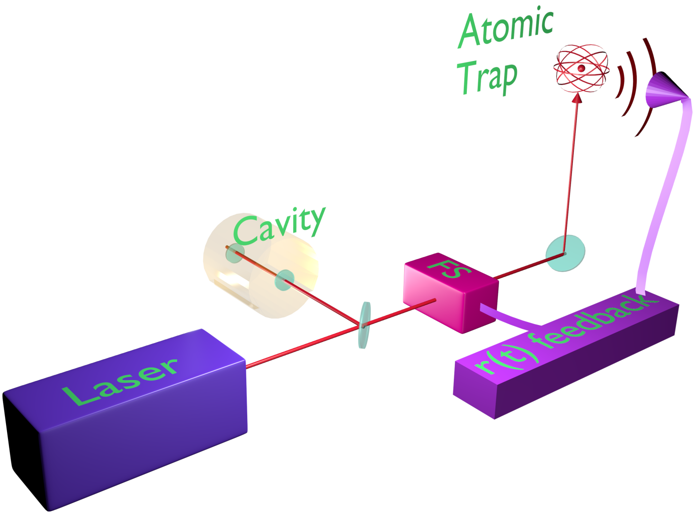

Optical atomic clocks

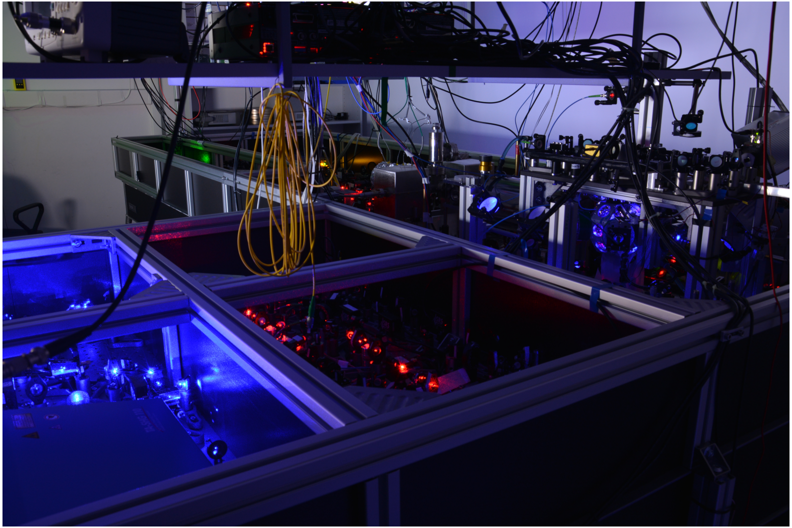

Optical atomic clocks

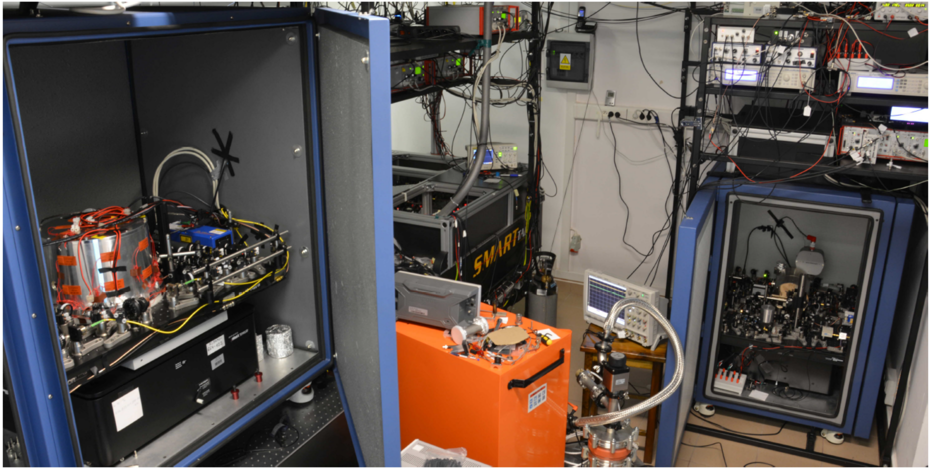

©Piotr Morzyński, KL FAMO, UMK, Poland

Optical atomic clocks - gravitational potential sensors

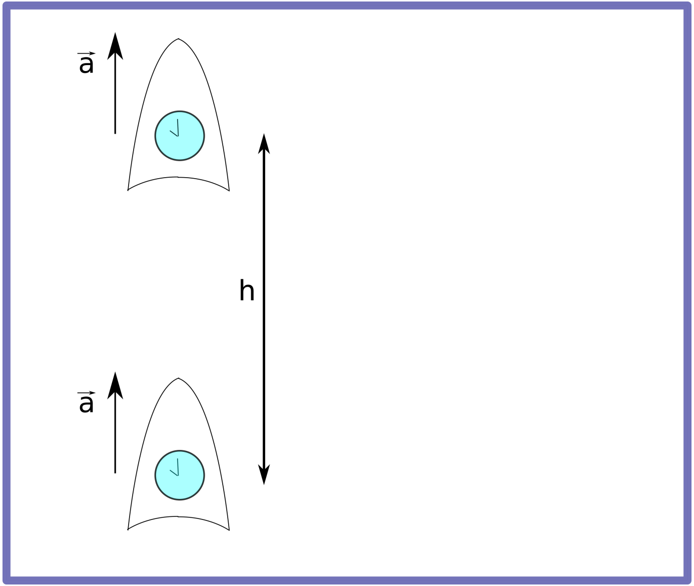

Optical atomic clocks - gravitational potential sensors

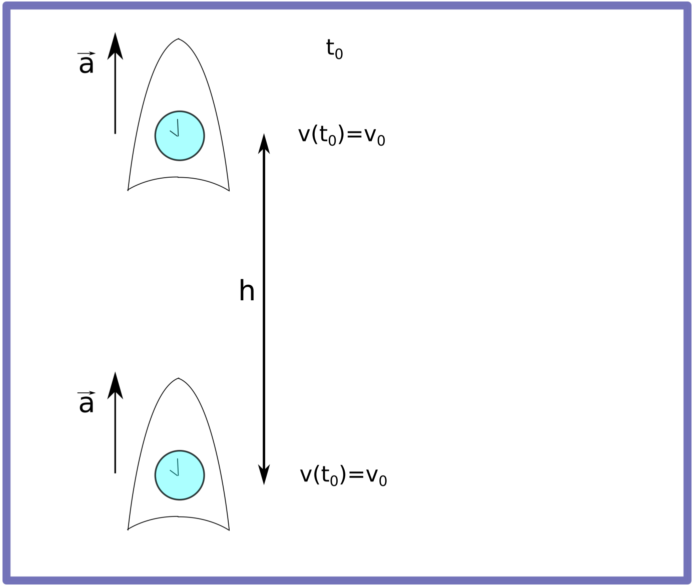

Optical atomic clocks - gravitational potential sensors

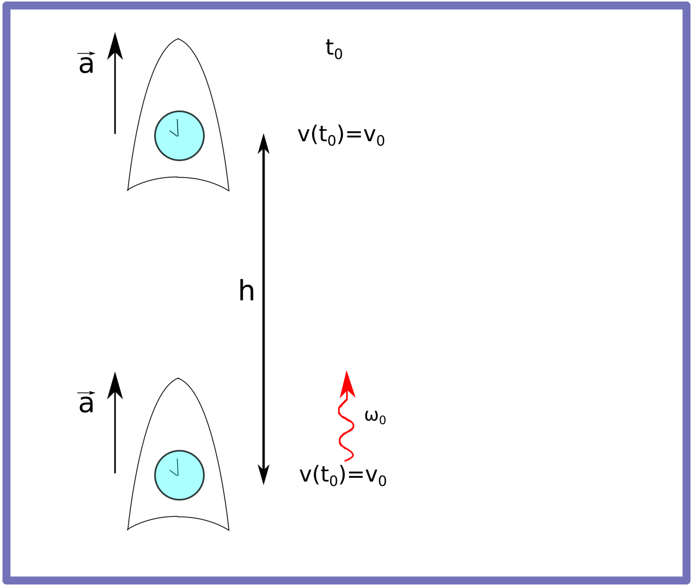

Optical atomic clocks - gravitational potential sensors

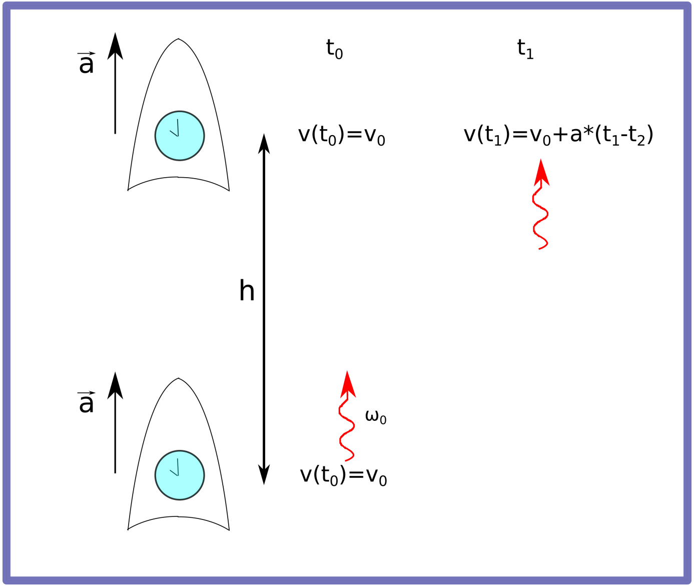

Optical atomic clocks - gravitational potential sensors

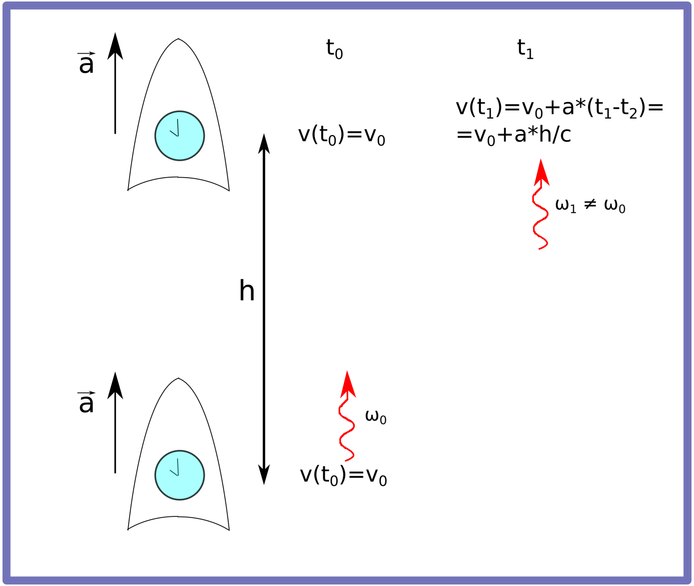

Optical atomic clocks - gravitational potential sensors

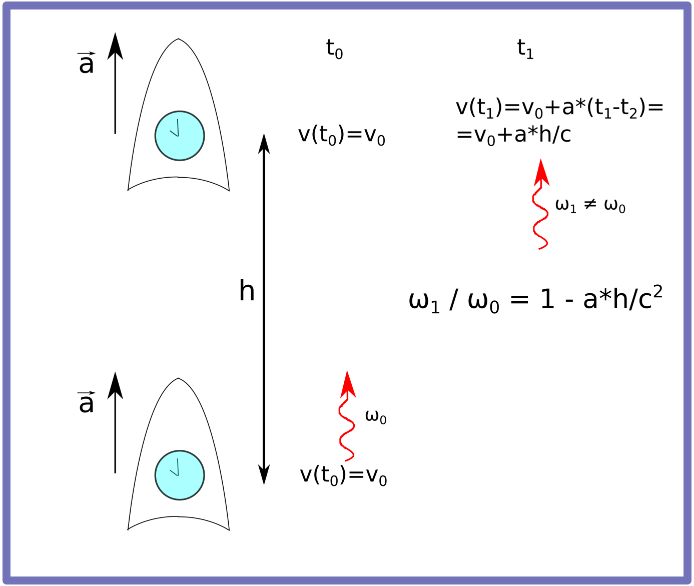

Optical atomic clocks - gravitational potential sensors

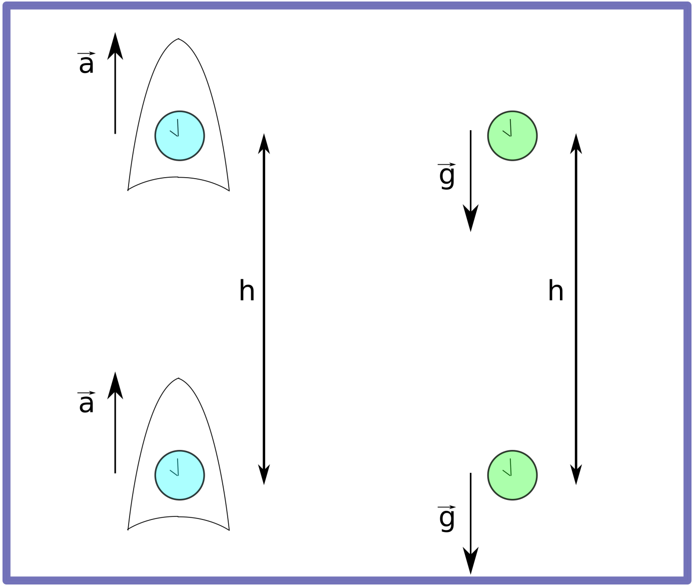

Optical atomic clocks - gravitational potential sensors

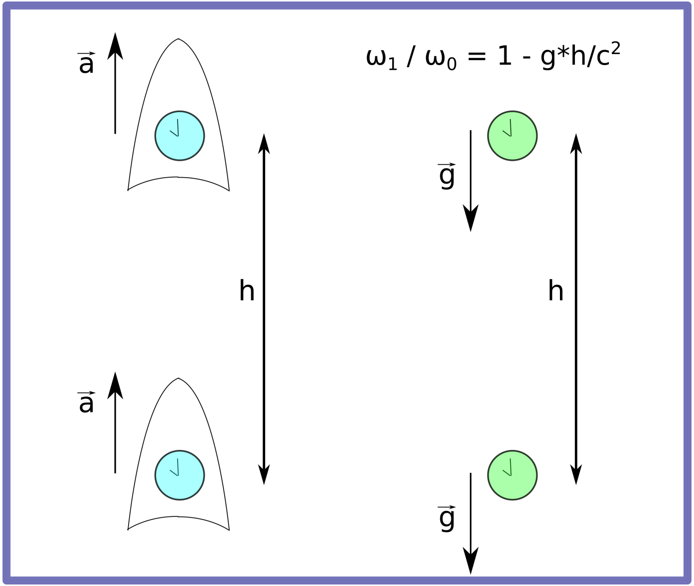

Gravitational redshift

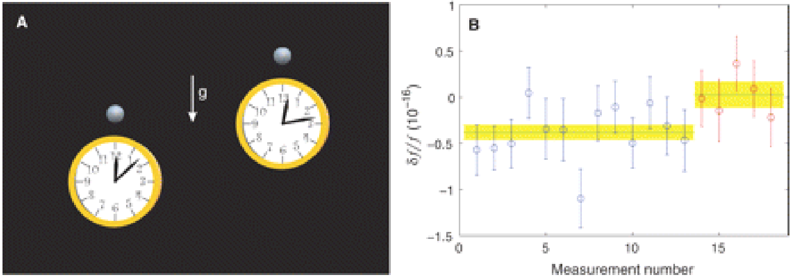

Clock raised by 33 cm - CW Chou, *et. al.*, Science, **329** 1630 (2010)

Gravitational redshift - land surveying

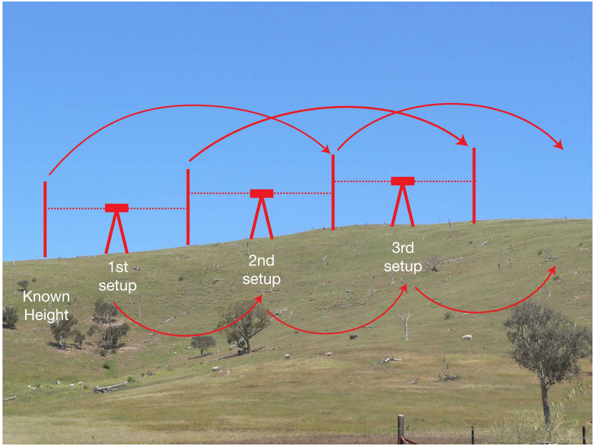

Gravitational redshift - land surveying - GRACE

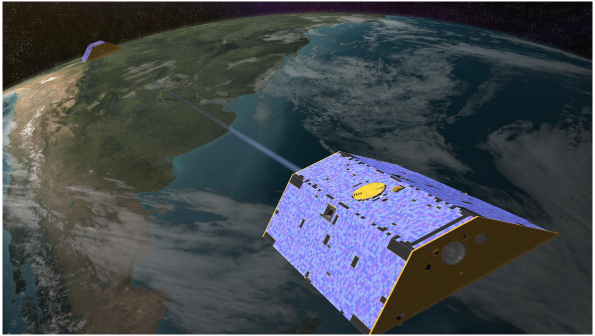

Source: NASA

Gravitational redshift - relativistic geodesy

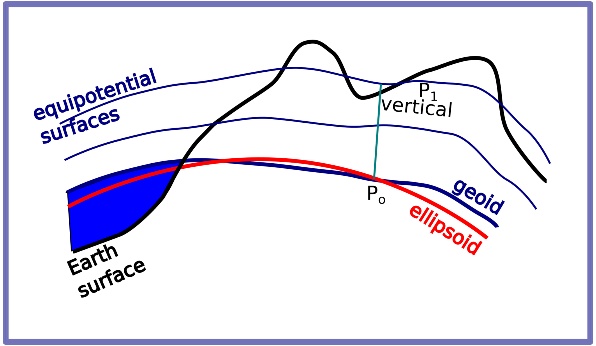

A. Bjerhammar, Bulletin Geodesique, **59** 207 (1985)

Gravitational redshift - relativistic geodesy

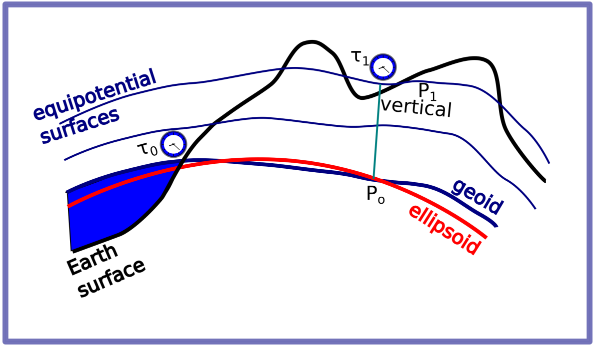

A. Bjerhammar, Bulletin Geodesique, **59** 207 (1985)

Gravitational redshift - fossils fuel hunt

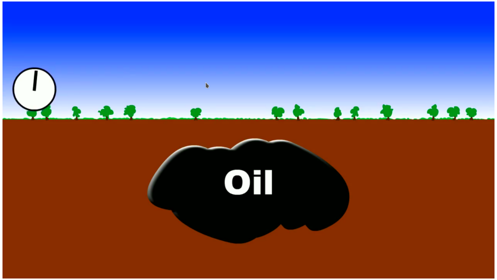

Courtesy of R. Bondarescu, M. Bondarescu and Media Team University of Zurich

Michał Zawada
KL FAMO, Nicolaus Copernicus University

Gravitational redshift - relativistic geodesy

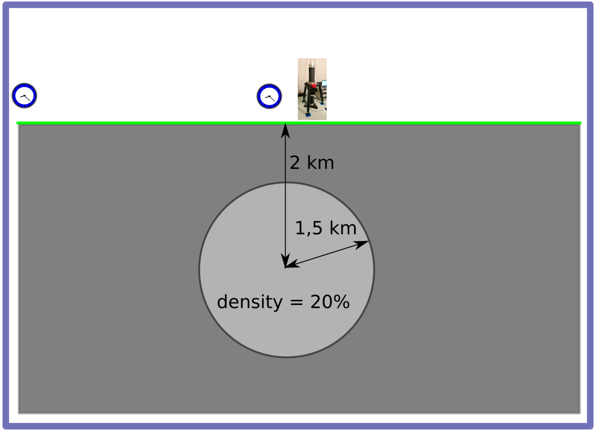

R. Bondarescu *et. al.* Geophys. J. Int. **191(1)** 78 (2012)

Gravitational redshift - relativistic geodesy

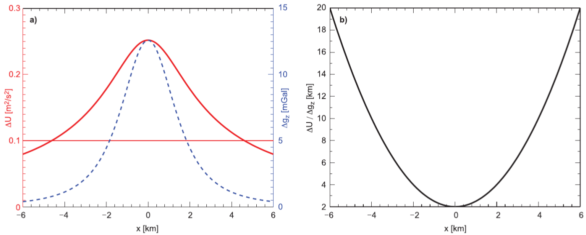

R. Bondarescu *et. al.* Geophys. J. Int. **191(1)** 78 (2012)

Gravitational redshift - groundwater level

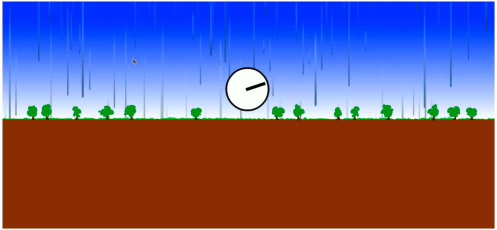

Gravitational redshift - volcano eruption

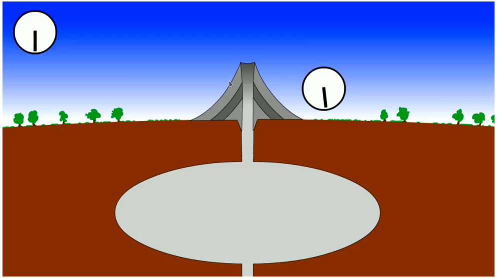

Gravitational redshift - volcano eruption

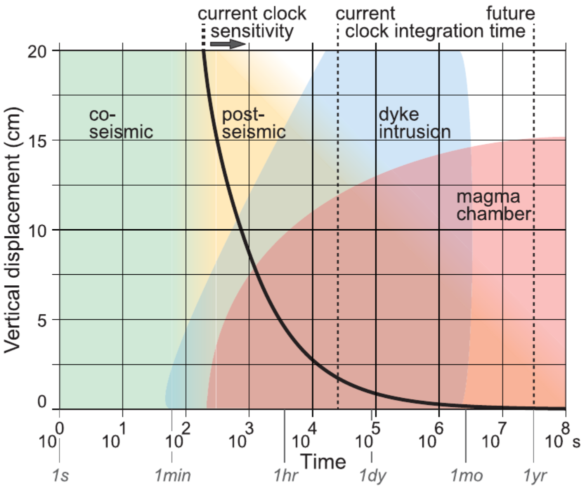

R. Bondarescu *et. al.* Geophys. J. Int. **191(1)** 78 (2012)

Gravitational redshift - THC

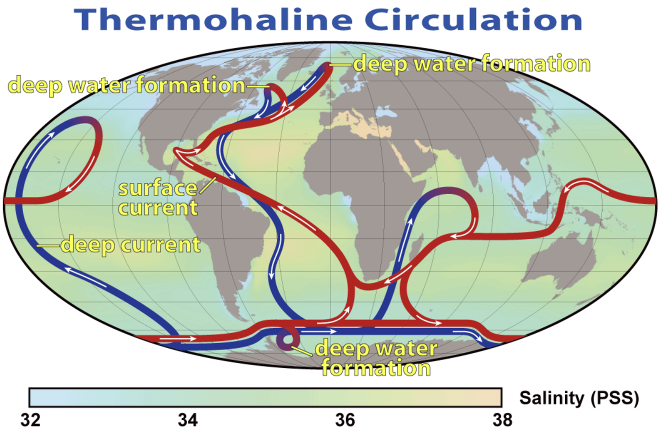

NASA Earth Observatory

Gravitational redshift - gravitational anomalies detection

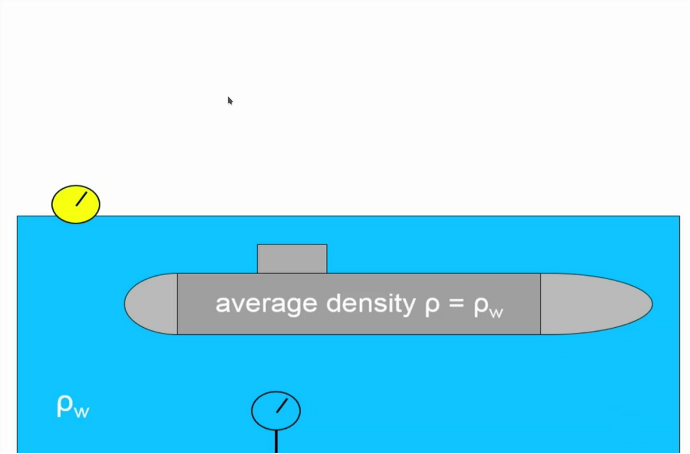

M. Bober and M. Zawada, Proc. SPIE 10438, https://doi.org/10.1117/12.2277402 (2017)

Gravitational redshift - gravitational anomalies detection

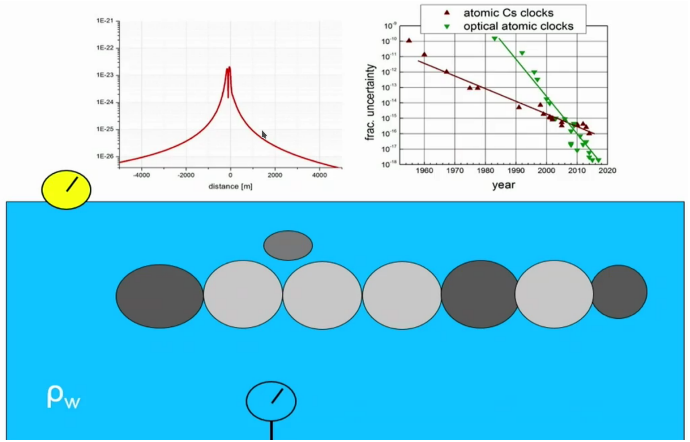

M. Bober and M. Zawada, Proc. SPIE 10438, https://doi.org/10.1117/12.2277402 (2017)

Lorentz invariance

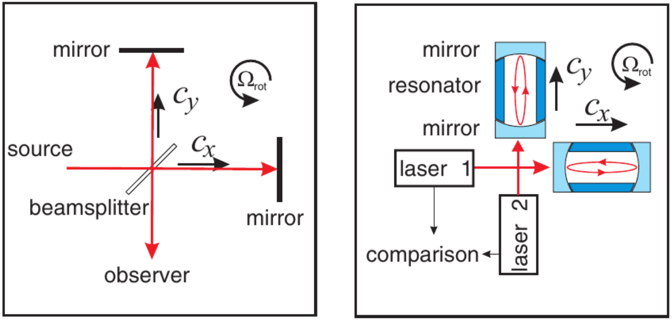

S. Herrmann *et al.*, Special Relativity. Lecture Notes in Physics, vol 702. Springer, Berlin, Heidelberg (2006)

Clocks on GPS constellation

PHYSICAL REVIEW A VOLUME 56, NUMBER 6 DECEMBER 1997

ARTICLES

Satellite test of special relativity using the global positioning system

Peter Wolf[1,2] and Gérard Petit[1]

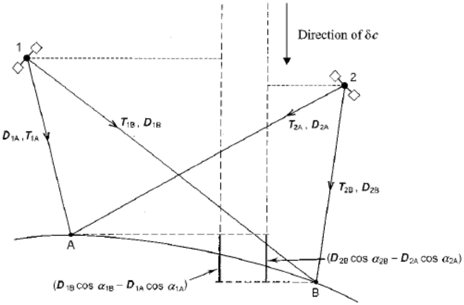

A clock network in Europe

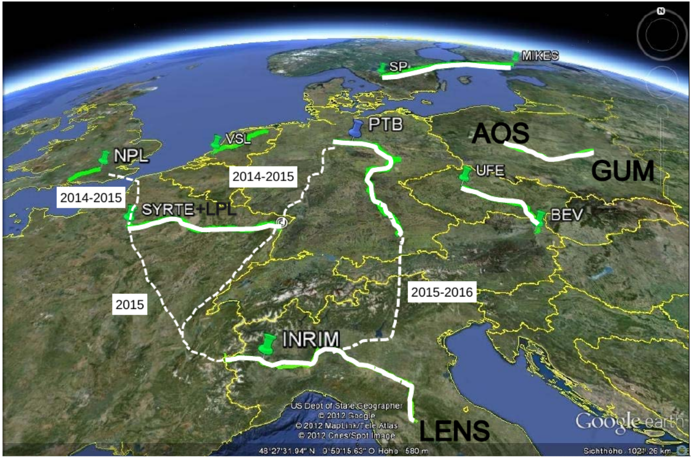

A clock network in Europe

19th International Congress of Metrology, 15001 (2019) https://doi.org/10.1051/metrology/201915001

The TiFOON Project – Time and Frequency Over Optical Networks

Jochen Kronjaeger, TiFOON Project Coordinator,
Time and Frequency Department,
National Physical Laboratory, Teddington, Middlesex TW11 0LW, UK

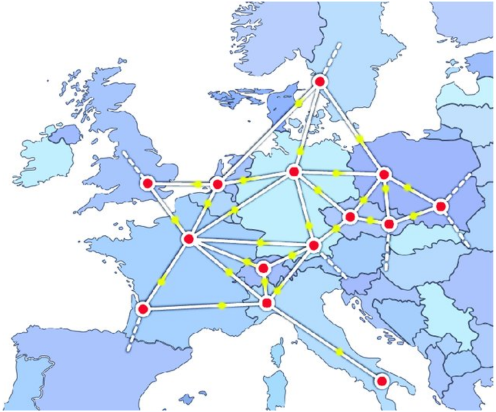

A clock network in Europe - LI

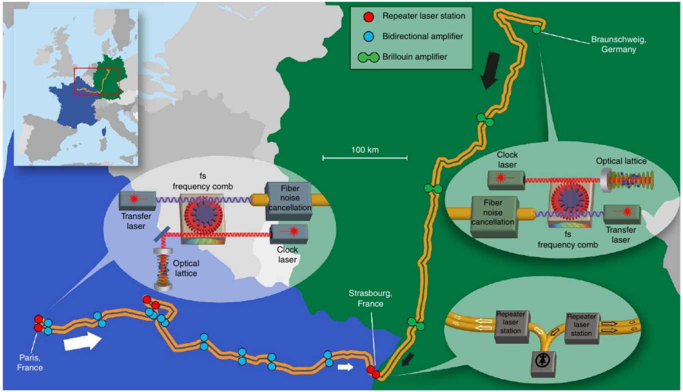

C. Lisdat, *et al.* Nat. Comm. **7** 12443 (2016)
P. Delva, *et al.* Phys. Rev. Lett. **118** 221102 (2017)

A clock on moving Earth - LI

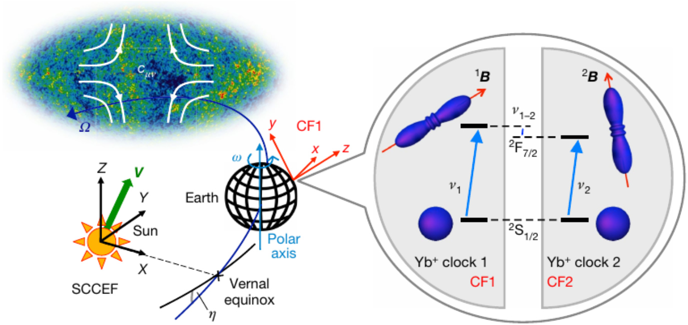

C. Sanner, *et al.* Nature **567** 204 (2019)

The problem with dark matter

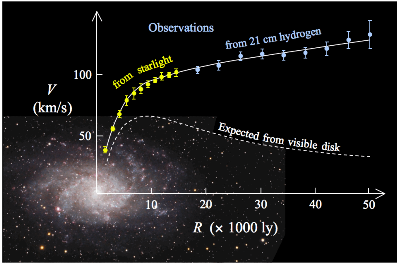

Picture from wikipedia by S. Deluca.

Data for the image are from Corbelli, E., and Salucci, P. (2000). *The extended rotation curve and the dark matter halo of M33*, MNRAS. 311 (2)

- Dark matter is non radiating, mostly non-barionic matter, which interacts very weakly with Standard Model matter.

The problem with dark matter

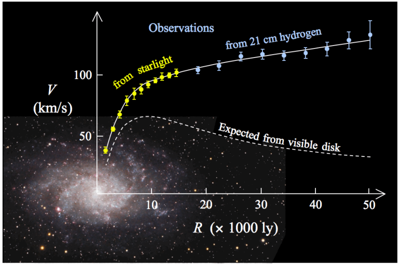

Picture from wikipedia by S. Deluca.

Data for the image are from Corbelli, E., and Salucci, P. (2000). *The extended rotation curve and the dark matter halo of M33*, MNRAS. 311 (2)

- Dark matter is non radiating, mostly non-barionic matter, which interacts very weakly with Standard Model matter.
- Density of dark matter (DM) in our galactic neighbourhood (observations of velocities of visible stars):

$$\rho_{cDM}^{local} \approx 0.4 \; GeV/cm^3$$

- Global dark matter density (WAMP):

$$\rho_{DM} = 1.3 \times 10^{-6} \; GeV/cm^3$$

- Inside the Solar System (planetary ephemerides-EPM2011):

$$\rho_{DM}^{Solar} < 10^5 \; GeV/cm^3$$

The problem with dark matter - range of masses

Working assumption - dark matter consists of particles

$$\rho_{DM} = m_{DM} * n_{DM}$$

Michał Zawada
KL FAMO, Nicolaus Copernicus University

The problem with dark matter - range of masses

Working assumption - dark matter consists of particles

$$\rho_{DM} = m_{DM} * n_{DM}$$

The inverse halo size of smallest galaxies:

$$10^{-22} eV < m_{DM}$$

The problem with dark matter - range of masses

Working assumption - dark matter consists of particles

$$\rho_{DM} = m_{DM} * n_{DM}$$

The inverse halo size of smallest galaxies:

$$10^{-22} eV < m_{DM}$$

The particles will not form black holes:

$$m_{DM} < 10^{28} eV$$

The problem with dark matter – WIMP

The most widely accepted hypothesis:
WIMP = Weakly interacting massive particles

Direct detection - collisions with nuclei.

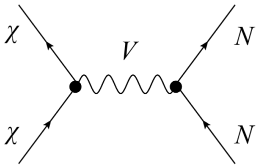

$$\mathcal{L}_{WIMP,eff} = \frac{e'_\chi e'_N}{4\pi} \frac{1}{M_V^2} (\overline{\chi}\gamma^\mu \chi)(\overline{N}\gamma_\mu N)$$

where $\overline{\chi} = \chi^\dagger \gamma^0$, and $\sigma_{scat} = \left(e'_\chi e'_N / M_V^2\right)^2$

The problem with dark matter – WIMP

The most widely accepted hypothesis:
WIMP = Weakly interacting massive particles

Direct detection - collisions with nuclei.

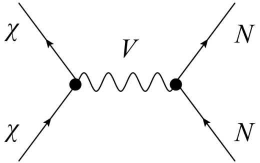

$$\mathcal{L}_{WIMP,eff} = \frac{e'_\chi e'_N}{4\pi} \frac{1}{M_V^2} (\overline{\chi}\gamma^\mu \chi)(\overline{N}\gamma_\mu N)$$

where $\overline{\chi} = \chi^\dagger \gamma^0$, and $\sigma_{scat} = (e'_\chi e'_N / M_V^2)^2$

experimentally (LUX): $\sigma_{scat} < 10^{-45}$ cm^2 !!!

Michał Zawada
KL FAMO, Nicolaus Copernicus University

The problem with dark matter - broadening the scope of DM searches

$$ToE \to \cdots \to GUT \to \cdots \to SU(3) \times SU(2) \times U(1)_Y \to SU(3) \times U(1)_{em}.$$

A scalar field

The most general form of self-interaction potential of a scalar field ϕ

$$V(\phi) = 2\frac{c^2}{\hbar^2} m_\phi^2 \phi^2 + \lambda\phi^4$$

- odd powers of ϕ field are ruled out because of symmetry $\phi \rightarrow -\phi$
- powers of ϕ^6 ad higher are ruled out because of renormalisation condition

Michał Zawada
KL FAMO, Nicolaus Copernicus University

A massive scalar field

$$V(\phi) = 2\frac{c^2}{\hbar^2} m_\phi^2 \phi^2 + \lambda \phi^4$$

A coherently oscillating classical field $\phi \sim \phi_0 \cos(\omega t + \delta)$

with Compton frequency $\omega = \frac{m_\phi c^2}{\hbar}$ $\rightarrow$ a valid DM candidate

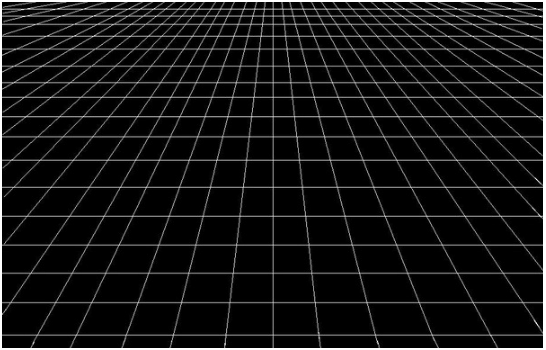

Michał Zawada
KL FAMO,
Nicolaus Copernicus University

A scalar field

$$V(\phi) = 2\frac{c^2}{\hbar^2} m_\phi^2 \phi^2 + \lambda\phi^4$$

If $m_\phi^2 < 0$ then the second term yields a spontaneous symmetry breaking and creation of topological solitons, otherwise called topological defects.

PHYSICS REPORTS (Review Section of Physics Letters) 121, No. 5 (1985) 263–315.

COSMIC STRINGS AND DOMAIN WALLS

Alexander VILENKIN

Phase transitions in Space - a spontaneous symmetry breaking

Example

Assume a field theory with a $G = U(1)$ group and a ϕ Higgs field with self-interaction potential $V(\phi)$:

$$V(\phi) = \frac{1}{2}\lambda(\phi^\dagger\phi - \eta^2)^2 = -\lambda\eta^2\phi^2 + \frac{1}{2}\lambda\phi^4 + \text{const},$$

where $\lambda > 1$ and ϕ field is complex.
$U(1)$ means a symmetry with respect of phase changes, $\phi \rightarrow e^{\hat{\imath}\alpha}\phi$

Phase transitions in Space - a spontaneous symmetry breaking

Example

Assume a field theory with a $G = U(1)$ group and a ϕ Higgs field with self-interaction potential $V(\phi)$:

$$V(\phi) = \frac{1}{2}\lambda(\phi^\dagger\phi - \eta^2)^2 = -\lambda\eta^2\phi^2 + \frac{1}{2}\lambda\phi^4 + \mathrm{const},$$

where $\lambda > 1$ and ϕ field is complex.

$U(1)$ means a symmetry with respect of phase changes, $\phi \rightarrow e^{\hat{\imath}\alpha}\phi$

The equation of motion of Lagrangian obey the symmetry.

Potential minima $V(\phi)$ (ground state of ϕ) are in non-zero values of ϕ, thus these solutions do not obey the symmetry, i.e.

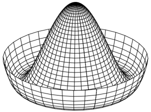

the symmetry is spontaneously broken.

Phase transitions in Space - a spontaneous symmetry breaking

Example

Assume a field theory with a $G = U(1)$ group and a ϕ Higgs field with self-interaction potential $V(\phi)$:

$$V(\phi) = \frac{1}{2}\lambda(\phi^\dagger\phi - \eta^2)^2 = -\lambda\eta^2\phi^2 + \frac{1}{2}\lambda\phi^4 + \text{const},$$

where $\lambda > 1$ and ϕ field is complex.

$U(1)$ means a symmetry with respect of phase changes, $\phi \to e^{\hat{\imath}\alpha}\phi$

The equation of motion of Lagrangian obey the symmetry.

Potential minima $V(\phi)$ (ground state of ϕ) are in non-zero values of ϕ, thus these solutions do not obey the symmetry, i.e.

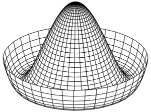

the symmetry is spontaneously broken.

ϕ has non-zero expectation value $\langle\phi\rangle = \eta e^{\hat{\imath}\theta}$, where only η is set by the model.

We have a manifold, M, of degenerate vacuum states corresponding to different choices of θ.

Phase transitions in Space - a spontaneous symmetry breaking

Example

Assume a field theory with a $G = U(1)$ group and a ϕ Higgs field with self-interaction potential $V(\phi)$:

$$V(\phi) = \frac{1}{2}\lambda(\phi^\dagger\phi - \eta^2)^2 = -\lambda\eta^2\phi^2 + \frac{1}{2}\lambda\phi^4 + \mathrm{const},$$

where $\lambda > 1$ and ϕ field is complex.
$U(1)$ means a symmetry with respect of phase changes, $\phi \to e^{\hat{\imath}\alpha}\phi$
Non-zero tempererature adds additional terms to the potential:

$$V_T(\phi) = AT^2\phi^\dagger\phi + V(\phi).$$

The effective mass of the field ϕ in temperature T

$$m^2(T) = AT^2 - \lambda\eta^2$$

is equal to zero in the critical temperature $T_c = \eta\sqrt{\lambda/A}$.

Phase transitions in Space - a spontaneous symmetry breaking

Example

Assume a field theory with a $G = U(1)$ group and a ϕ Higgs field with self-interaction potential $V(\phi)$:

$$V(\phi) = \frac{1}{2}\lambda(\phi^\dagger\phi - \eta^2)^2 = -\lambda\eta^2\phi^2 + \frac{1}{2}\lambda\phi^4 + \mathrm{const},$$

where $\lambda > 1$ and ϕ field is complex.
$U(1)$ means a symmetry with respect of phase changes, $\phi \to e^{\hat{\imath}\alpha}\phi$
Non-zero tempererature adds additional terms to the potential:

$$V_T(\phi) = AT^2\phi^\dagger\phi + V(\phi).$$

The effective mass of the field ϕ in temperature T

$$m^2(T) = AT^2 - \lambda\eta^2$$

is equal to zero in the critical temperature $T_c = \eta\sqrt{\lambda/A}$.
If $T > T_c$ then $m^2(T)$ is positive and the minimum of $V_T(\phi)$ is in $\phi = 0$.
The expectation value of ϕ vanishes and the symmetry is restored.

Cosmic phase transitions

What is happening as the universe cools through T_c?

The field ϕ will tend to develop an expectation value $\langle\phi\rangle$ corresponding to some point in the manifold M.
Since all points in M are equivalent, the choice will depend on random fluctuations and will be different in different regions of space.

Cosmic phase transitions

For the sake of simplicity let's take a real field ϕ and

$$\mathcal{L} = \frac{1}{2}\left(\partial_\mu \phi\right)^2 - \frac{1}{2}\mu^2\phi^2 - \frac{1}{4}\lambda\phi^4.$$

Cosmic phase transitions

For the sake of simplicity let's take a real field ϕ and

$$\mathcal{L} = \frac{1}{2}\left(\partial_\mu \phi\right)^2 - \frac{1}{2}\mu^2\phi^2 - \frac{1}{4}\lambda\phi^4.$$

The symmetry is $Z_2 : \phi \to -\phi$, the minima of $V(\phi)$ are in $\phi = \pm\sqrt{\frac{-\mu^2}{\lambda}} \equiv \pm\eta$, and so manifold M consists of only two points.

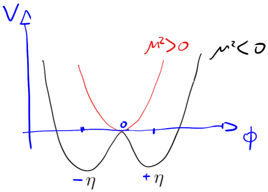

Cosmic phase transitions

For the sake of simplicity let's take a real field ϕ and

$$\mathcal{L} = \frac{1}{2}\left(\partial_\mu \phi\right)^2 - \frac{1}{2}\mu^2\phi^2 - \frac{1}{4}\lambda\phi^4.$$

The symmetry is $Z_2 : \phi \to -\phi$, the minima of $V(\phi)$ are in $\phi = \pm\sqrt{\frac{-\mu^2}{\lambda}} \equiv \pm\eta$, and so manifold M consists of only two points.

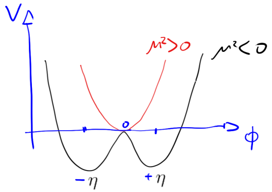

As we go from a region with $\langle\phi\rangle = +\eta$ to a region with $\langle\phi\rangle = -\eta$, we must pass through $\langle\phi\rangle = 0$, therefore these two regions are separated by a domain wall of false vacuum.

Cosmic phase transitions

After the phase transition $\langle\phi\rangle$ will be different in different regions of space.

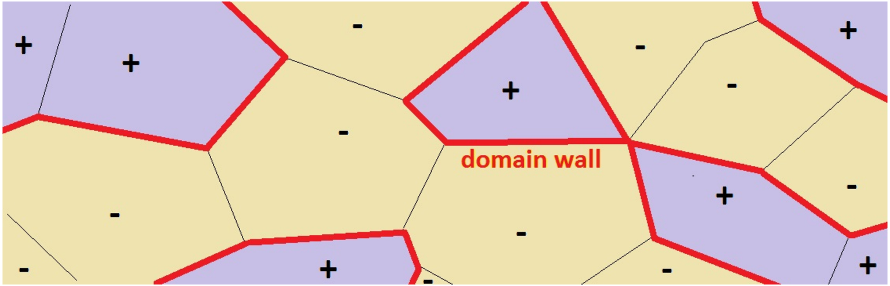

Picture from MIT by Trung Van Phan

Size of domains is determined by the correlation length $\xi \sim T_C^{-1}$
and restricted by an event horizon - the Kibble-Żurek mechanism with speed c

Topological defects

Plethora of topological defects:

- Domain walls
- Strings
- Monopols
- Monopols connected by strings
- Walls bounded by strings
- ...

Topological defects carry energy and are comparable in size to the Compton wavelength $d \sim m^{-1}$ of vector and Higgs bosons of a given field $\rightarrow$ another valid DM candidate

Michał Zawada
KL FAMO, Nicolaus Copernicus University

A scalar field ϕ

$$V(\phi) = 2\frac{c^2}{\hbar^2} m_\phi^2 \phi^2 + \lambda \phi^4$$

can couple to SM by different "portals", for instance:

$$\mathcal{L}_{scalar}^{lin} = \frac{\phi}{\Lambda_\gamma} \frac{\mathcal{F}_{\mu\nu}\mathcal{F}^{\mu\nu}}{4} - \sum_f \frac{\phi}{\Lambda_f} m_f \bar{f} f + \sum_V \frac{\phi}{\Lambda_V} \frac{M_V^2}{2} V_\nu V^\nu$$

$$\mathcal{L}_{scalar}^{quad} = \frac{\phi^2}{(\Lambda'_\gamma)^2} \frac{\mathcal{F}_{\mu\nu}\mathcal{F}^{\mu\nu}}{4} - \sum_f \frac{\phi^2}{(\Lambda'_f)^2} m_f \bar{f} f + \sum_V \frac{\phi^2}{(\Lambda'_V)^2} \frac{M_V^2}{2} V_\nu V^\nu$$

Λ_γ (Λ'_γ) and Λ_f (Λ'_f) are the energy scales of the respective linear (quadratic) couplings.

Coupling to QED

$$\mathcal{L}_{QED} = \hat{\imath}\hbar c\overline{\psi_e}\gamma^\mu D_\mu \psi_e - m_e c^2 \overline{\psi_e}\psi_e + \frac{1}{4\mu_0}\mathcal{F}_{\mu\nu}\mathcal{F}^{\mu\nu}$$

where m_e i ψ_e are mass and field of electron, respectively, $\alpha = \frac{\mu_0}{4\pi}\frac{e^2 c}{\hbar}$

Coupling to QED

$$\mathcal{L}_{QED} = \hat{\imath}\hbar c\overline{\psi_e}\gamma^{\mu}D_{\mu}\psi_e - m_e c^2\overline{\psi_e}\psi_e + \frac{1}{4\mu_0}\mathcal{F}_{\mu\nu}\mathcal{F}^{\mu\nu}$$

where m_e i ψ_e are mass and field of electron, respectively, $\alpha = \frac{\mu_0}{4\pi}\frac{e^2 c}{\hbar}$

$$\mathcal{L}^{lin}_{scalar,int} = \frac{\phi}{\Lambda_\gamma}\frac{\mathcal{F}_{\mu\nu}\mathcal{F}^{\mu\nu}}{4} - \sum_f \frac{\phi}{\Lambda_f} m_f \bar{f} f \longrightarrow \frac{\phi}{\Lambda_\gamma}\frac{\mathcal{F}_{\mu\nu}\mathcal{F}^{\mu\nu}}{4\mu_0} - \frac{\phi}{\Lambda_e} m_e c^2\overline{\psi_e}\psi_e$$

$$\mathcal{L}^{quad}_{scalar,int} = \frac{\phi^2}{(\Lambda'_\gamma)^2}\frac{\mathcal{F}_{\mu\nu}\mathcal{F}^{\mu\nu}}{4} - \sum_f \frac{\phi^2}{(\Lambda'_f)^2} m_f \bar{f} f \longrightarrow \frac{\phi^2}{(\Lambda'_\gamma)^2}\frac{\mathcal{F}_{\mu\nu}\mathcal{F}^{\mu\nu}}{4\mu_0} - \frac{\phi^2}{(\Lambda'_e)^2} m_e c^2\overline{\psi_e}\psi_e$$

Coupling to QED

$$\mathcal{L}_{QED} = \hat{\imath}\hbar c\overline{\psi_e}\gamma^\mu D_\mu \psi_e - m_e c^2 \overline{\psi_e}\psi_e + \frac{1}{4\mu_0}\mathcal{F}_{\mu\nu}\mathcal{F}^{\mu\nu}$$

where m_e i ψ_e are mass and field of electron, respectively, $\alpha = \frac{\mu_0}{4\pi}\frac{e^2 c}{\hbar}$

$$\alpha \to \frac{\alpha}{1-\phi/\Lambda_\gamma} \simeq \alpha\left(1+\frac{\phi}{\Lambda_\gamma}\right), \frac{\delta m_e}{m_e} = \frac{\phi}{\Lambda_e}$$

$$\alpha \to \frac{\alpha}{1-\phi^2/(\Lambda'_\gamma)^2} \simeq \alpha\left(1+\frac{\phi^2}{(\Lambda'_\gamma)^2}\right), \frac{\delta m_e}{m_e} = \frac{\phi^2}{(\Lambda'_e)^2}$$

Observed values of α and m_e will change because of coupling to ϕ

Effective α and m_e variations due to dark matter scalar fields

Different forms of scalar fields ϕ yield different α and m_e variations:

- basic excitations of ϕ - oscillating field - α and m_e oscillate with field's Compton frequency,
- basic excitations of ϕ - oscillating field - slow drift of α and m_e (time average of $\langle\phi\rangle \sim \phi_0/2$),
- topological defects created in phase transitions in early Universe - transient-in-time variation of α and m_e.

Effective α and m_e variations due to dark matter scalar fields

Different forms of scalar fields ϕ yield different α and m_e variations:

- basic excitations of ϕ - oscillating field - α and m_e oscillate with field's Compton frequency,
- basic excitations of ϕ - oscillating field - slow drift of α and m_e (time average of $\langle\phi\rangle \sim \phi_0/2$),
- topological defects created in phase transitions in early Universe - transient-in-time variation of α and m_e.

Effective α oscillations due to dark matter scalar fields

Two frequency references

- different locations

Effective α oscillations due to dark matter scalar fields

Two frequency references

- different locations
- different sensitivities

Effective α oscillations due to dark matter scalar fields

Two frequency references

- different locations
- different sensitivities

The electronic part of the Schrödinger equation within the Born-Oppenheimer approximation, in SI units, in dimensionless form, for n electrons and m nuclei:

$$\left(-\frac{1}{2}\sum_{i=1}^{n}\nabla^2_{x_i} - \sum_{i,j=1}^{n,m}\frac{Z_j}{x_{ji}} + \frac{1}{2}\sum_{\substack{i,k=1\\ i\neq k}}^{n,n}\frac{1}{x_{ik}}\right)\psi = \epsilon\psi,$$

where $\epsilon = E/E_h$ and $x_i = r_i/a_0$, with $E_h = \alpha^2 m_e c^2$ and $a_0 = \hbar/(m_e \alpha c)$.

Effective α oscillations due to dark matter scalar fields

Two frequency references

- different locations
- different sensitivities

The electronic part of the Schrödinger equation within the Born-Oppenheimer approximation, in SI units, in dimensionless form, for n electrons and m nuclei:

$$\left(-\frac{1}{2}\sum_{i=1}^{n} \nabla^2_{x_i} - \sum_{i,j=1}^{n,m} \frac{Z_j}{x_{ji}} + \frac{1}{2} \sum_{\substack{i,k=1 \\ i \neq k}}^{n,n} \frac{1}{x_{ik}} \right)\psi = \epsilon\psi,$$

where $\epsilon = E/E_h$ and $x_i = r_i/a_0$, with $E_h = \alpha^2 m_e c^2$ and $a_0 = \hbar/(m_e \alpha c)$.

$$E \propto \alpha^2 \qquad L \propto \alpha^{-1}$$

PRL **114**, 161301 (2015) PHYSICAL REVIEW LETTERS week ending 24 APRIL 2015

Searching for Dark Matter and Variation of Fundamental Constants with Laser and Maser Interferometry

Y. V. Stadnik* and V. V. Flambaum†

Magnetometry - two isotopes with different sign of sensitivity

PRL 115, 011802 (2015) PHYSICAL REVIEW LETTERS week ending 3 JULY 2015

Search for Ultralight Scalar Dark Matter with Atomic Spectroscopy

Ken Van Tilburg,[1,*] Nathan Leefer,[2,†] Lykourgos Bougas,[2,‡] and Dmitry Budker[2–4,§]

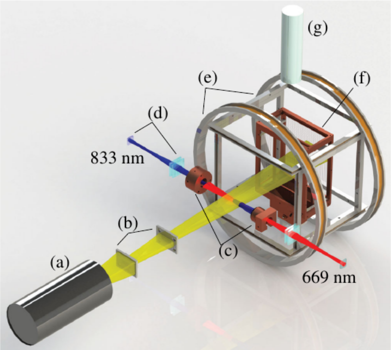

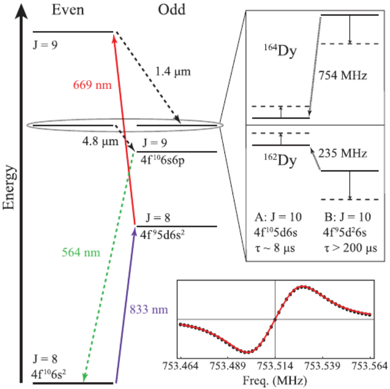

Magnetometry - two isotopes with different sign of sensitivity

PRL **115**, 011802 (2015) PHYSICAL REVIEW LETTERS week ending 3 JULY 2015

Search for Ultralight Scalar Dark Matter with Atomic Spectroscopy

Ken Van Tilburg,[1,*] Nathan Leefer,[2,†] Lykourgos Bougas,[2,‡] and Dmitry Budker[2–4,§]

The strength of the linear coupling d_e is the inverse of the energy scale Λ_γ.

$$d_e = \frac{M_P c^2}{\sqrt{4\pi}\Lambda_{\gamma,1}}$$

where $M_P c^2 = 1.2 \times 10^{19}$ GeV is the Planck mass energy equivalent.

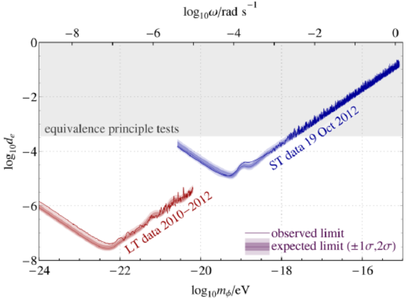

Atomic fountain - two species with different clock frequency

PRL 117, 061301 (2016) PHYSICAL REVIEW LETTERS week ending 5 AUGUST 2016

Searching for an Oscillating Massive Scalar Field as a Dark Matter Candidate Using Atomic Hyperfine Frequency Comparisons

A. Hees,[1,2,*] J. Guéna,[1,†] M. Abgrall,[1,‡] S. Bize,[1,§] and P. Wolf[1,||]

II. THE FO2-RB ATOMIC FOUNTAIN

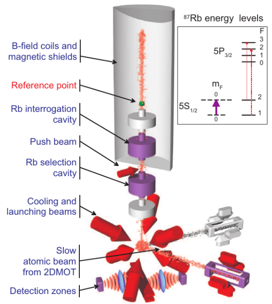

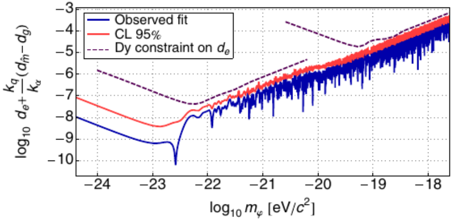

$$d_{\hat{m}} = \frac{d_{m_u} m_u + d_{m_d} m_d}{m_u + m_d}$$

source: J Guéna *et al* 2014 Metrologia 51 108

Optical atomic clock - two components with different sensitivity

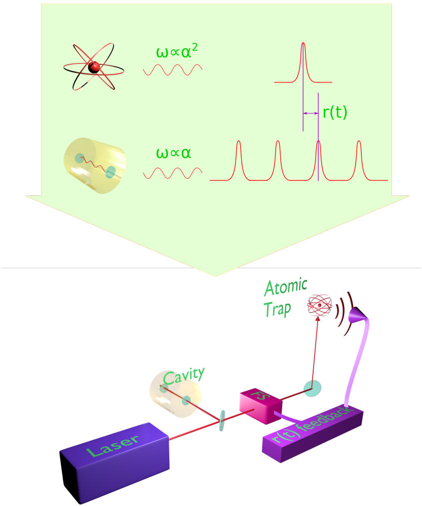

- $E \propto \alpha^2 \Rightarrow \omega_0^{at} \propto \alpha^2$
  with relativistic effects
  $E \propto \alpha^2 \Rightarrow \omega_0^{at} \propto \alpha^{(2+k_\alpha^{at})}$
- $L \propto \alpha^{-1}$
  $\Rightarrow \omega_0^{cav} = N_{cav} c/(2L) \propto \alpha^1$

Optical atomic clock - two components with different sensitivity

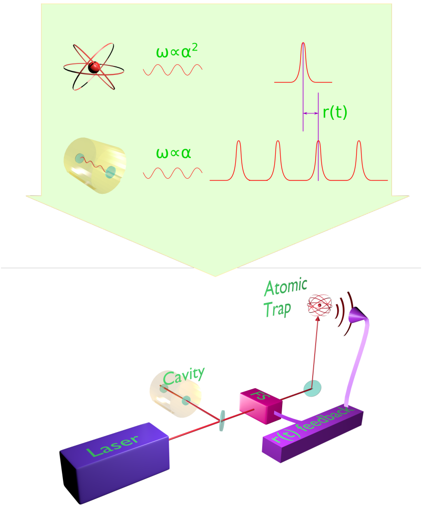

- $E \propto \alpha^2 \Rightarrow \omega_0^{at} \propto \alpha^2$
  with relativistic effects
  $E \propto \alpha^2 \Rightarrow \omega_0^{at} \propto \alpha^{(2+k_\alpha^{at})}$
- $L \propto \alpha^{-1}$
  $\Rightarrow \omega_0^{cav} = N_{cav} c/(2L) \propto \alpha^1$

$$d\omega_0 = \omega_0(2 + k_\alpha^{at} - 1)\frac{d\alpha}{\alpha}$$
$$= \omega_0(1 + k_\alpha^{at})\frac{d\alpha}{\alpha}$$
$$\equiv \omega_0 K_\alpha \frac{d\alpha}{\alpha}$$

Optical atomic clock - two components with different sensitivity

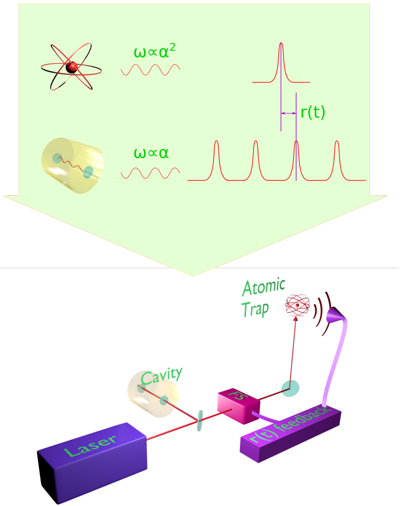

- $E \propto \alpha^2 \Rightarrow \omega_0^{at} \propto \alpha^2$
  with relativistic effects
  $E \propto \alpha^2 \Rightarrow \omega_0^{at} \propto \alpha^{(2+k_\alpha^{at})}$
- $L \propto \alpha^{-1}$
  $\Rightarrow \omega_0^{cav} = N_{cav} c/(2L) \propto \alpha^1$

$$d\omega_0 = \omega_0(2 + k_\alpha^{at} - 1)\frac{d\alpha}{\alpha}$$
$$= \omega_0(1 + k_\alpha^{at})\frac{d\alpha}{\alpha}$$
$$\equiv \omega_0 K_\alpha \frac{d\alpha}{\alpha}$$

The variations of α can be seen in the feedback signal $r(t)$

P. Wcisło, et al. ***Nature Astronomy*** **1 0009 (2016)**

Optical atomic clock - two components with different sensitivity

For each frequency of the oscillation ω, i.e. for each mass m_ϕ, the $R(t) = B + A(\omega)cos(\omega t + \delta)$ function is fitted to the normalised signals.

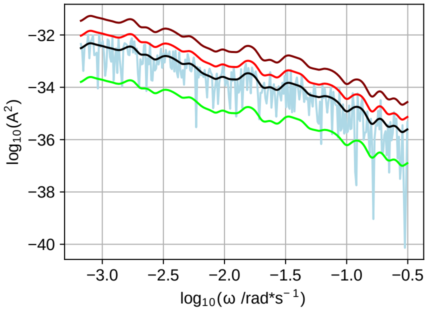

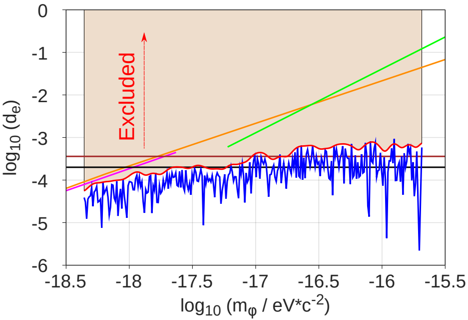

P. Wcisło, et al. *Sci. Adv.* 4 eaau4869 (2018)

Transient-in-time variation of effective α

PHYSICS REPORTS (Review Section of Physics Letters) 121, No. 5 (1985) 263–315.

COSMIC STRINGS AND DOMAIN WALLS

Alexander VILENKIN

$$V(\phi) = 2\frac{c^2}{\hbar^2} m_\phi^2 \phi^2 + \lambda\phi^4$$

where $m_\phi^2 < 0$

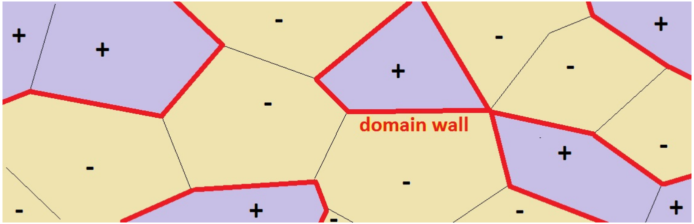

Picture from MIT by Trung Van Phan

Transient-in-time variation of effective α

Nature Physics **10**, 933–936 (2014)

Hunting for topological dark matter with atomic clocks

A. Derevianko and M. Pospelov

$$\frac{d\omega_0}{\omega_0} = k_\alpha \frac{d\alpha}{\alpha}$$

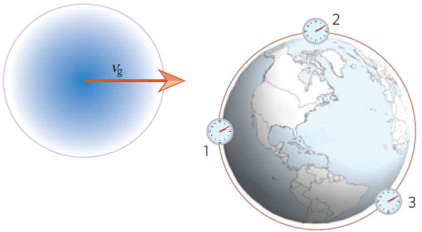

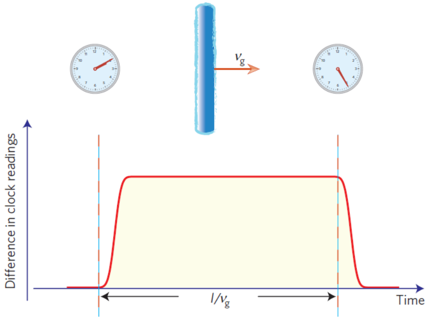

Transient-in-time variation of effective α

Nature Physics **10**, 933–936 (2014)

Hunting for topological dark matter with atomic clocks

A. Derevianko and M. Pospelov

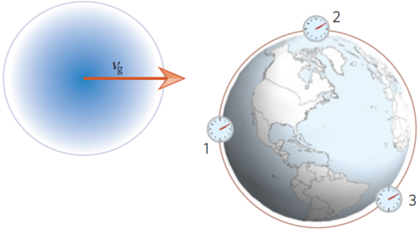

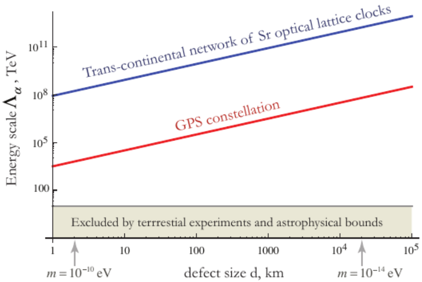

Microwave clocks on GPS constellation

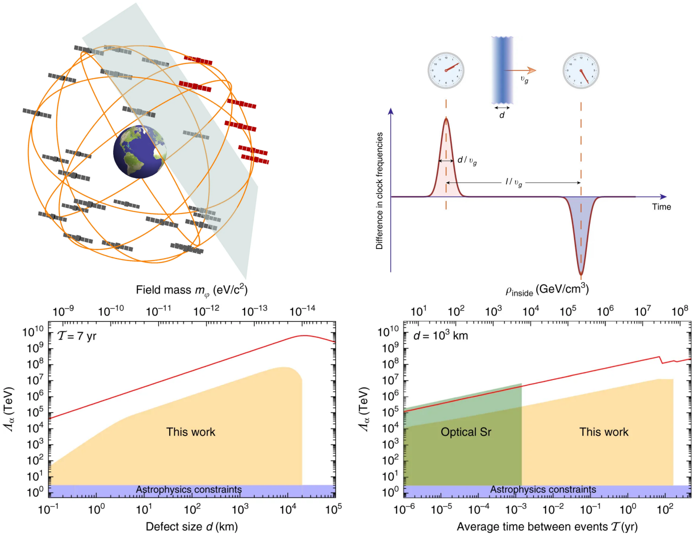

B. M. Roberts, et al. *Nat. Commun.* **8** 1195 (2017)

Intercontinental network of optical atomic clocks.

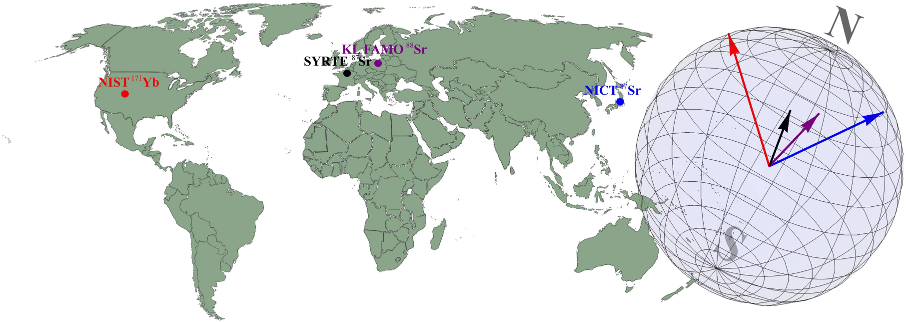

The readouts of the distant clocks do not need to be correlated in real time. Just as in the standard radio-astronomical technique, very-long-baseline interferometry, they can be locally recorded (with time stamps that are accurate to the level of 1 ms) and cross-correlated later.

Observation campaign made from archival data

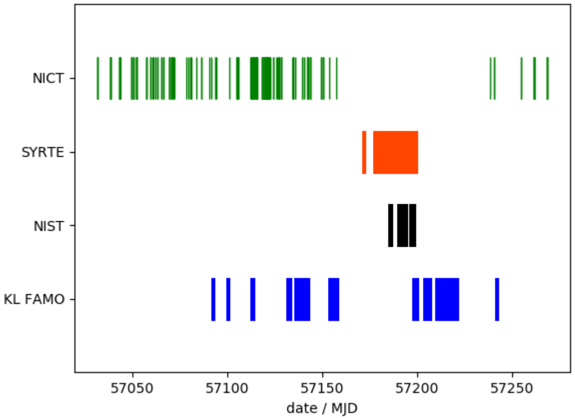

Observation sessions spanning Jan. 2015 to Dec. 2015.

Supplement - how the correlation in VLBI works?

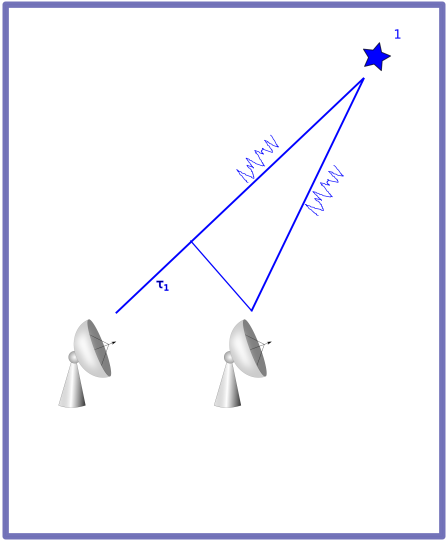

Supplement - how the correlation in VLBI works?

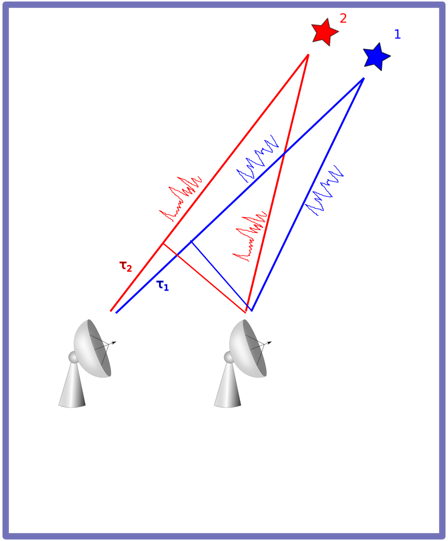

Supplement - how the correlation in VLBI works?

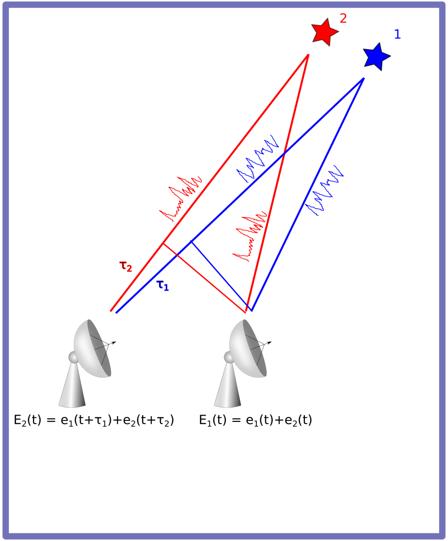

Supplement - how the correlation in VLBI works?

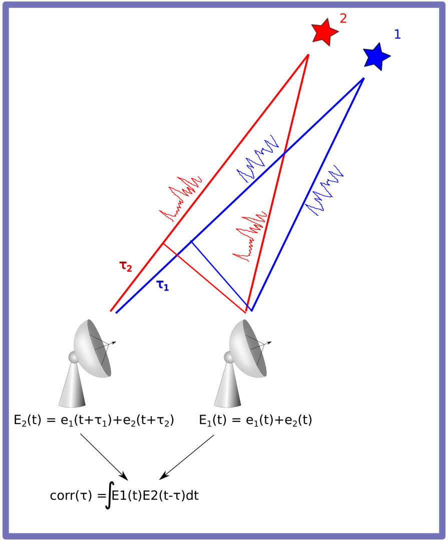

Supplement - how the correlation in VLBI works?

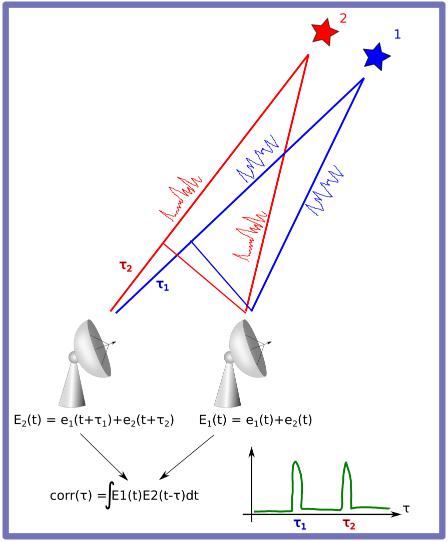

Topological defects

The transient effect can be detected by cross-correlating the pairs of feedbacks $r_i(t)$ recorded in the network of worldwide dispersed clocks.

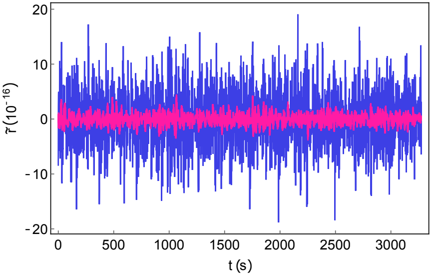

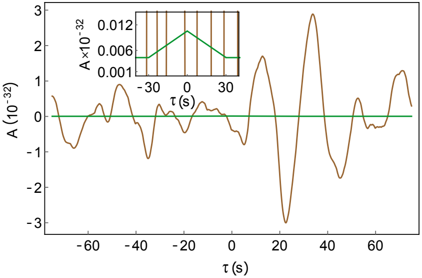

The expected cross-correlation shape is fitted to cross-correlated data.

Topological defects

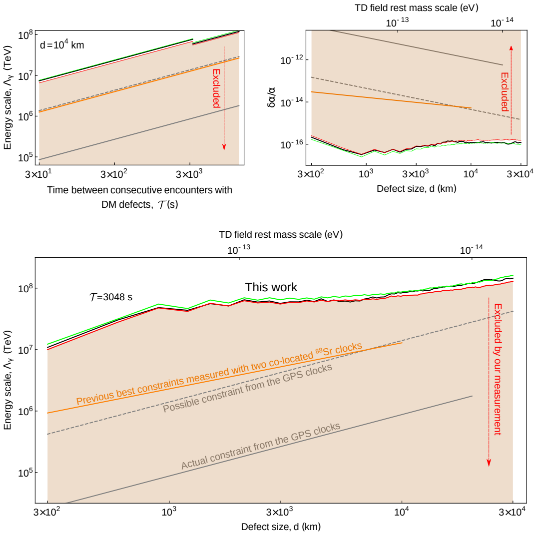

The topological defect size comparable to the size of the Earth (10,000 km) $\Rightarrow$
$\delta\alpha/\alpha < 1.6 \times 10^{-16}$.

Coupling to SM mass

Constraining domain wall dark matter with a network of superconducting gravimeters and LIGO

Rees L. McNally* and Tanya Zelevinsky

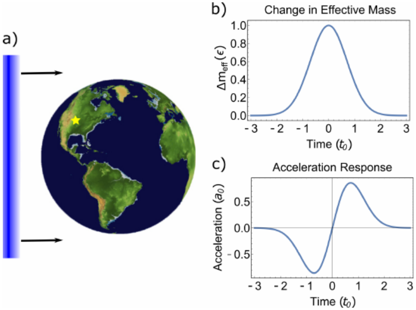

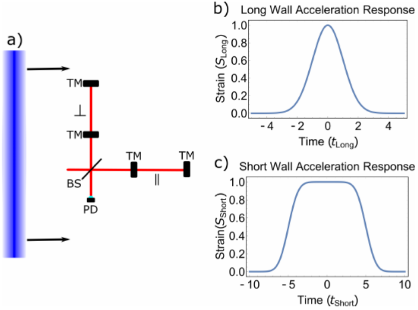

Coupling to SM mass

Constraining domain wall dark matter with a network of superconducting gravimeters and LIGO

Rees L. McNally* and Tanya Zelevinsky

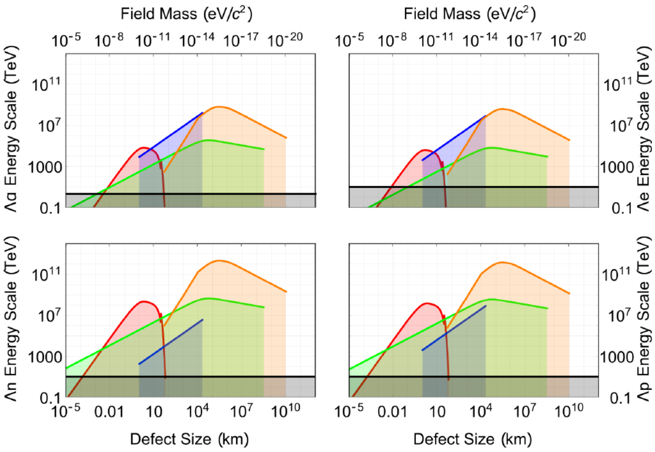

Coupling to SM

Search for New Physics with Atoms and Molecules

M.S. Safronova[1,2], D. Budker[3,4,5], D. DeMille[6], Derek F. Jackson Kimball[7], A. Derevianko[8] and Charles W. Clark[2]

Spin	Type	Operator	Interaction	DM effects	Searches
0	scalar	$\varphi\, h^\dagger h,\ \phi^n\, \mathcal{O}_{\rm SM}$	Higgs portal / dilaton	fund.-constant variation	Atomic clocks, GPS.DM
		$a\, G^{\mu\nu}\tilde{G}_{\mu\nu}$	axion-QCD	nucleon EDM	CASPEr-Electric
	pseudo-scalar	$a\, F^{\mu\nu}\tilde{F}_{\mu\nu}$	axion-E&M	EMF along B field	ADMX, CULTASK, MADMAX
		$(\partial_\mu a)\bar{\psi}\gamma^\mu\gamma_5\psi$	axion-fermion	spin torque	CASPEr-Wind, GNOME, QUAX
1	vector	$F'_{\mu\nu}F^{\mu\nu}$	vector–photon mixing	EMF in vacuum	DM Radio, ADMX
		$F'_{\mu\nu}\bar{\psi}\sigma^{\mu\nu}\psi$	dipole operator	spin torque	CASPEr-Wind
	axial-vector	$A'_\mu\bar{\psi}\gamma^\mu\gamma^5\psi$	minimally coupled	spin torque	CASPEr-Wind

Passive optical atomic clock

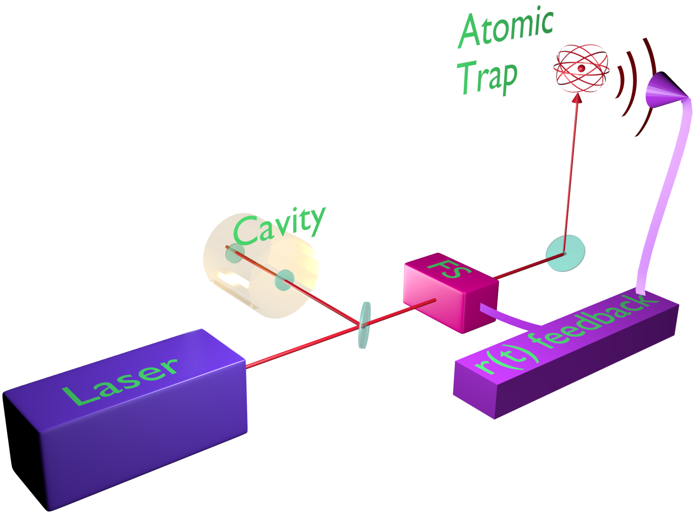

Michał Zawada
KL FAMO, Nicolaus Copernicus University

Passive vs active atomic clock

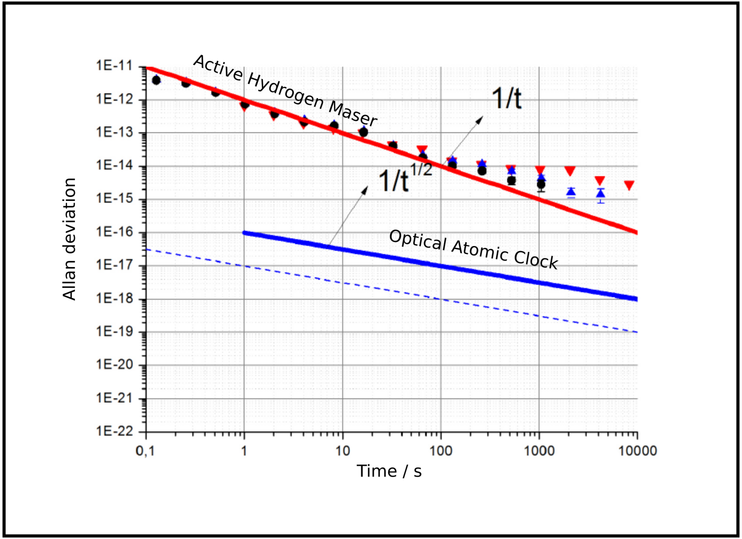

Passive vs active atomic clock

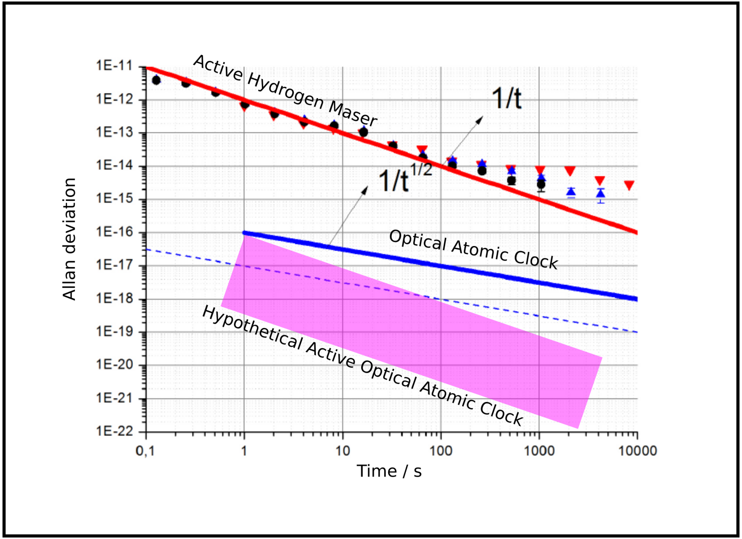

Passive vs active atomic clock

Higgs force in atoms

What is the origin of electron, and up and down quarks masses?
The Higgs coupling form SM:

$$y_e^{SM}(m_h) \approx 2.0 \times 10^{-6}, y_u^{SM}(m_h) \approx 5.4 \times 10^{-6}, y_d^{SM}(m_h) \approx 1.1 \times 10^{-6},$$

Michał Zawada
KL FAMO, Nicolaus Copernicus University

Higgs force in atoms

What is the origin of electron, and up and down quarks masses?
The Higgs coupling form SM:

$$y_e^{SM}(m_h) \approx 2.0 \times 10^{-6}, y_u^{SM}(m_h) \approx 5.4 \times 10^{-6}, y_d^{SM}(m_h) \approx 1.1 \times 10^{-6},$$

Indirect LHC bounds (from Higgs decay, status as of 2015)

$$y_e < 1.3 \times 10^{-3}, y_{u,d} < 1.3 \times 10^{-2}$$

Higgs-mediated force in atoms

PHYSICAL REVIEW D **96**, 093001 (2017)

Probing atomic Higgs-like forces at the precision frontier

Cédric Delaunay,[1,*] Roee Ozeri,[2,†] Gilad Perez,[3,‡] and Yotam Soreq[4,§]

Higgs boson exchange between a nucleus of mass number A and one of its bound electrons induces an attractive potential of Yukawa type:

$$V_{Higgs}(r) = -\frac{y_e y_A}{4\pi}\frac{e^{-rm_h}}{r}$$

Higgs force - attractive, the higher l state, the less is affected

$$\delta E^{Higgs}_{nlm} = \langle nlm|V_{Higs}|nlm\rangle \approx - -\frac{y_e y_A}{4\pi m_h^2}|\phi(0)|^2\frac{\delta l,0}{n^3}$$

How to measure the Higgs force? Change the total mass not changing the total charge.

Kings plot

W. H. King, Isotope Shifts in Atomic Spectra (Springer, 1984).

$$\delta\nu_i^{A'A} = \frac{A' - A}{AA} MS_i + \delta\langle r^2\rangle^{A'A} E_i$$

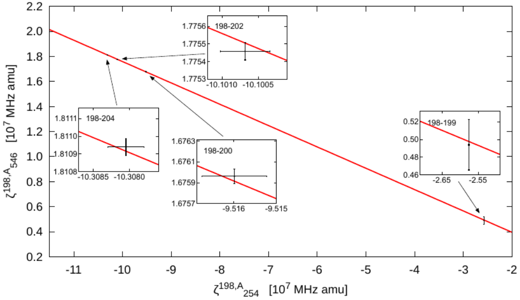

M. Witkowski *et. al.* Opt. Express 27 11069 (2019)

Kings plot

W. H. King, Isotope Shifts in Atomic Spectra (Springer, 1984).

$$\delta\nu_i^{A'A} = \frac{A' - A}{AA} MS_i + \delta\langle r^2\rangle^{A'A} E_i$$

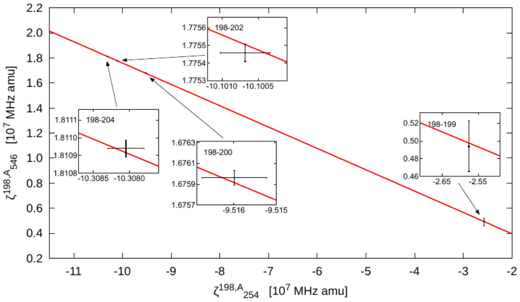

M. Witkowski *et. al.* Opt. Express 27 11069 (2019) The Higgs give non-linear contributions

Thank you for your attention!

iqClock
QUANTUM FLAGSHIP
EMPIR
EURAMET
The EMPIR initiative is co-funded by the European Union's Horizon 2020 research and innovation programme and the EMPIR Participating States

Fundusze Europejskie Inteligentny Rozwój
Rzeczpospolita Polska
FNP Fundacja na rzecz Nauki Polskiej
Unia Europejska Europejski Fundusz Rozwoju Regionalnego